Transverse form factors of ^{117}Sn

H. Baghaei,* J. Dubach, M. B. Frodyma,† R. S. Hicks, R. A. Miskimen, G. A. Peterson, and S. H. Rokni‡
Department of Physics and Astronomy, University of Massachusetts, Amherst, Massachusetts 01003

A. Hotta
Department of Liberal Arts, School of Physics, Shizuoka University, Shizuoka, Japan

T. Suzuki
Department of Physics, Nihon University, Setagaya, Tokyo 156, Japan
(Received 21 April 1993)

Transverse elastic and inelastic form factors for low-lying levels in ^{117}Sn have been measured by 180° electron scattering in the momentum transfer range q_{eff}=1.1–2.4 fm^{-1}. The simple independent-particle model fails to account for these data, predicting form factors that are much too large. In better quantitative agreement with the data are the results of more detailed calculations that allow for configuration mixing of valence nucleons, as well as first-order core polarization. As in the similar case of ^{205}Tl, these calculations successfully predict the presence of a deep diffraction minimum observed in the intermediate q region of the elastic $M1$ form factor. Nevertheless, the overall description of the data by the detailed calculations remains quantitatively unsatisfactory. A more complete understanding of these data may rely upon the consideration of multiparticle-multihole configurations outside the $0\hbar\omega$ basis space.

PACS number(s): 25.30.Bf, 25.30.Dh, 27.60.+j

I. INTRODUCTION

Although the independent-particle model (IPM) has been remarkably successful in describing a vast range of nuclear properties, the predictions of this model for various magnetic properties are usually only in qualitative agreement with data. With regard to magnetic dipole ($M1$) properties, for example, isovector moments predicted by the IPM deviate systematically from observed values, and calculated electromagnetic form factors often exceed measurements by factors of 2 or more. Various explanations have been proposed for these differences, including in-shell configuration mixing, core polarization (CP) involving higher-excited single-particle levels, meson exchange currents (MEC's), and Δ-isobar excitations.

Electron scattering measurements [1] of the elastic $M1$ form factors of ^{207}Pb and ^{205}Tl provided new insight into the effects of CP in massive nuclei. The $J^{\pi} = \frac{1}{2}^{-}$ and $J^{\pi} = \frac{1}{2}^{+}$ ground states of ^{207}Pb and ^{205}Tl result from unpaired nucleon holes in the $3p_{1/2}$ neutron and $3s_{1/2}$ proton valence orbits of the ^{208}Pb core. Owing to the $n = 3$ nodal quantum number, as well as to the small orbital ℓ values, the wave functions of both these valence orbits have large amplitudes within the interior of the nucleus. Thus polarization effects on these orbitals will involve the entire nuclear volume to a far greater extent than for nuclei with valence nucleons in large ℓ, $n = 1$ orbitals, which are concentrated at the nuclear surface. Consequently, ^{207}Pb and ^{205}Tl are especially favorable nuclei for studying the full effects of CP. Papanicolas *et al.* [1] showed that the $M1$ form factor of ^{207}Pb is uniformly smaller than mean-field predictions by a factor of 2 within the $1.3 < q_{\mathrm{eff}} < 2.6$ fm^{-1} momentum transfer range of their measurements. The reduction observed for ^{205}Tl was even more marked, corresponding to a factor of about 3.

According to theoretical studies [2, 3], much of this quenching can be attributed to first-order CP. The more realistic of these calculations [3] employed the Michigan three-range Yukawa (M3Y) effective interaction [4]. One-pion and ρ-meson exchange currents were also included [5]. However, for the momentum transfer range of the available data, the largest modifications to the IPM predictions came from CP. The calculations of Suzuki *et al.* [3, 5] remedied many of the problems observed with the mean-field results. For example, the reduced magnitude of the $M1$ form factor in ^{207}Pb was satisfactorily explained. Perhaps the most remarkable success of these calculations was their prediction of a deep minimum observed near $q_{\mathrm{eff}} = 1.5$ fm^{-1} in the $M1$ form factor of ^{205}Tl. In the calculations this minimum results from a dramatic cancellation between the independent-particle matrix element and CP terms arising primarily from the tensor force in the effective interaction.

On the other hand, CP calculations failed to predict

*Present address: Department of Physics, University of Virginia, Charlottesville, VA 22901.

†Present address: Saddleback College, Division of Mathematics and Science, Mission Viejo, CA 92692.

‡Present address: Stanford Linear Accelerator Center, Stanford University, Stanford, CA 94309.

0556-2813/93/48(2)/735(8)/$06.00

the extent of the observed quenching of the diffraction maximum near $q_{\rm eff} = 2\ {\rm fm}^{-1}$ in the ^{205}Tl form factor. Although some quenching was obtained in this region, the calculated form factor still exceeded the measurements by a factor of 2. In part, this can be attributed [1] to the neglect of mixing between the different configurations made possible by the presence of two neutron holes in addition to the $3s_{1/2}$ proton hole in the ^{208}Pb core. The resultant configuration mixing decreases the amplitude of the $3s_{1/2} \otimes |0^+>_{204}$ component in the ^{205}Tl ground state, leading to a further reduction of the predicted $M1$ form factor. However, Papanicolas *et al.* [1] argued that there exists an even more fundamental problem stemming from the customary reliance of CP calculations on the assumption of a closed-shell core. Indeed, the occupation of the ^{208}Pb core orbits is expected to be diminished by the presence of ground state correlations [6]. By introducing these correlations into nuclear matter descriptions [6, 7], the occupation probability of orbits just below the Fermi energy has been estimated to be about 0.7. Such an occupancy is not inconsistent with the quenching of the elastic magnetic form factors measured by Papanicolas *et al.* [1]. More generally, partial occupancy of the shell-model orbits is considered [6] to be responsible for the systematic overestimation by mean-field calculations of the single-particle transition strength for nuclei in the vicinity of ^{208}Pb, as well as for the predictions of central charge densities of the lead isotopes larger than those observed experimentally.

Here we report the first measurements of the transverse elastic form factor of ^{117}Sn, another $J^\pi = \frac{1}{2}^+$ nucleus. Results from particle-transfer reactions [8, 9] suggest that the dominant configuration in the ^{117}Sn ground state has an unpaired neutron in the $3s_{1/2}$ orbit. Thus ^{117}Sn is propitious for further examining the interpretation of the strong quenching observed in the $M1$ form factor of ^{205}Tl. *A priori*, it is not clear that similar CP effects would be expected. In ^{205}Tl the $3s_{1/2}$ valence particle is a proton, and both the proton and neutron shells are almost full. On the other hand, whereas the ^{117}Sn proton shell is closed, the valence $3s_{1/2}$ neutron orbit lies midway between the $N = 50$ and $N = 82$ major shell closures. The interpretation of the ^{117}Sn results should therefore include shell-model evaluations of configuration mixing within the $0\hbar\omega$ neutron shell, as well as first-order CP calculations of excitations beyond that space.

In addition to the elastic $M1$ form factor of ^{117}Sn, form factors have been measured for transverse excitation of states at 0.159 MeV ($J^\pi = \frac{3}{2}^+$), 0.317 MeV ($J^\pi = \frac{11}{2}^-$), 0.712 MeV ($J^\pi = \frac{7}{2}^+$), 1.01 MeV ($J^\pi = \frac{3}{2}^+, \frac{5}{2}^+$ doublet), and 1.18 MeV ($J^\pi = \frac{5}{2}^+$), as well as for excitations to multiplets at 1.45 and 1.57 MeV. These transitions appear to have appreciable single-particle character, and therefore provide additional tests of the suitability of the various structure models.

II. EXPERIMENTAL DETAILS AND DATA ANALYSIS

The experiment was performed with the 180° electron scattering facility [10] of the Bates-MIT Linear Accelerator Center. By atomic number, the main constituents of the target were 84.2% ^{117}Sn and 9.4% ^{118}Sn; the remaining 6.4% was comprised mainly of ^{116}Sn, ^{119}Sn, and ^{120}Sn. This 29.2-mg/cm^2-thick foil was supported by a massive copper frame cooled by alcohol to $-40\,^\circ$C so that average beam currents as large as 35 μA could be utilized without melting the target. Electrons scattered through 180° were deflected into a high-resolution 900 MeV/c magnetic spectrometer [11].

Spectra were measured up to an excitation energy of 3 MeV for eight different incident electron energies E_0 ranging from 100.1 to 221.2 MeV. Cross sections were extracted by line-shape fitting the measured spectra and applying corrections for radiative and ionization effects. Details of the analysis procedures have been given elsewhere [12]. Fitted spectra for E_0=120.6 and 170.8 MeV are shown in Fig. 1. The magnitudes of the deduced cross sections were checked against measurements of elastic scattering from the proton, for which absolute cross sections are known [13] to an accuracy of 2% in the kinematic range of the present experiment. For these measurements a rotating polyethylene target was employed.

Coulomb scattering is minimized at 180°, but nevertheless still contributes to the measured cross sections

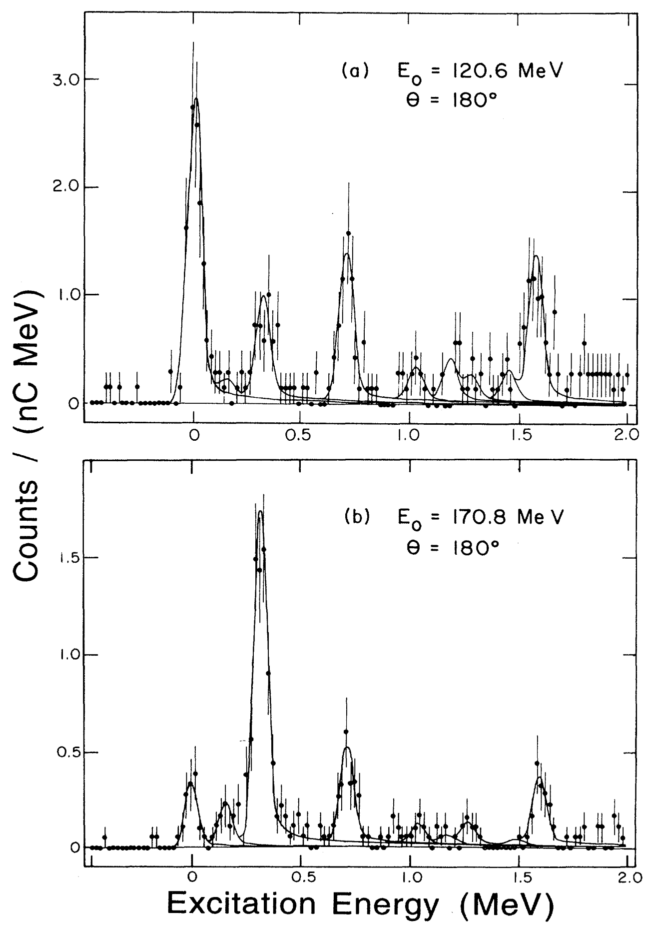

FIG. 1. Line-shape fits for spectra measured at θ=180° for beam energies of (a) E_0 = 120.6 MeV and (b) 170.8 MeV.

due to the finite acceptance solid angle of the spectrometer and multiple scattering in the target [14]. At the three lowest incident beam energies, such contributions to elastic scattering were accounted for by measuring the elastic Coulomb cross section of ^{92}Mo at 180° under conditions identical to those of the ^{117}Sn measurements. Magnetic elastic scattering is forbidden for the $J^\pi = 0^+$ nucleus ^{92}Mo. Coulomb cross sections for the Sn target were then obtained [15] by multiplying the measured ^{92}Mo cross sections by ratios of form factors for elastic Coulomb scattering from Sn and ^{92}Mo, calculated in the distorted-wave Born approximation (DWBA) from the respective well-known charge densities [16, 17]. The DWBA calculations were performed at the effective scattering angle [14] $\theta_{\rm eff}$, which, for this experiment, ranged from 177.80° to 178.90°, depending mainly on the entrance slit size of the spectrometer.

At higher beam energies the elastic cross section of ^{92}Mo could not be measured with sufficient statistical precision to permit such analyses. For these cases we relied upon DWBA calculations of the Sn Coulomb cross sections. Comparisons at the three lowest beam energies of the measured and calculated ^{92}Mo cross sections indicated that Coulomb cross sections obtained in this way are accurate to about 25%. Coulomb contributions to the measured elastic cross sections were 80% at E_0=100 MeV and 42.6% at 121 MeV, but less than 5% for beam energies of 171 MeV and higher. For the elastic measurements at 141 and 161 MeV, Coulomb contributions were found to account for essentially all the observed cross sections, indicating that the elastic magnetic form factor has a deep diffraction minimum near $q_{\rm eff}$=1.6 fm^{-1}. Table I shows values deduced for the transverse elastic form factor by means of the relation [15]

$$F_T^2(q) = \left(\frac{2k}{Z\alpha}\right)^2 \eta \, \frac{d\sigma}{d\Omega} \ ,$$

where Z is the nuclear charge, k the momentum of the incident electron, and the differential cross section is corrected for Coulomb scattering. The parameter η is a recoil factor, for 180° scattering equal to $(1 + 2k/M)$, where M is the target atomic mass.

Table I also lists inelastic form factors deduced for the peaks observed at 0.159, 0.317, 0.712, 1.01, 1.18, 1.45, and 1.57 MeV. According to $0\hbar\omega$ shell-model descriptions, these excited states are primarily formed by rearrangement within the partially filled neutron shell. Hence Coulomb scattering corrections should be small. Furthermore, with the possible exception of the last two of these excitations, the 9.4% ^{118}Sn contaminant in the target presents no difficulty because its first excited state lies at an excitation energy of 1.23 MeV.

III. THEORETICAL MODELS

As previously noted, CP calculations for ^{117}Sn are more involved than those for ^{205}Tl or ^{207}Pb. In the latter cases, the doubly magic closed-shell "core" is well defined. For ^{117}Sn, $Z = 50$ corresponds to a closed proton shell, but the $3s_{1/2}$ neutron of interest lies in the middle of the $1g_{7/2}2d_{5/2}2d_{3/2}3s_{1/2}1h_{11/2}$ neutron shell where the energy spacings between the various single-particle levels are relatively small. For ^{205}Tl and ^{207}Pb, the IPM provides a reasonable starting point; for ^{117}Sn, however, the most naive use of the IPM would give a ground-state neutron configuration of $1g^{8\nu}_{7/2}2d^{6\nu}_{5/2}2d^{3\nu}_{3/2}$, and thereby predict the wrong ground-state spin.

For these reasons, we have examined a variety of models to describe the structure of ^{117}Sn and the corresponding elastic and inelastic form factors. Four such models will be used in the discussion and interpretation of the results in the next section. The first simply takes the most obvious IPM configuration that gives the correct ground-state spin, $1g^{8\nu}_{7/2}2d^{6\nu}_{5/2}2d^{2\nu}_{3/2}3s^{1\nu}_{1/2}$. The second approach adds CP on top of this simple IPM configuration. The M3Y interaction (neglecting the small spin-orbit term) was used, and all first-order CP contributions were included. Because the calculations required that the CP be built on top of closed j shells, ^{117}Sn was calculated as the (coherent) average of ^{115}Sn ($1g^{8\nu}_{7/2}2d^{6\nu}_{5/2}3s^{1\nu}_{1/2}$) and ^{119}Sn ($1g^{8\nu}_{7/2}2d^{6\nu}_{5/2}2d^{4\nu}_{3/2}3s^{1\nu}_{1/2}$). While this approach closely resembles that for ^{205}Tl and ^{207}Pb, it may be less reliable for an open-shell nucleus such as ^{117}Sn. In particular,

TABLE I. Experimentally deduced transverse form factors of ^{117}Sn, multiplied by 10^8. Percentage uncertainties are shown within parentheses; values expressed as upper limits are assessed on the basis of three standard deviations. Contributions from longitudinal scattering have been subtracted from the ground-state results. For other transitions, longitudinal contributions are estimated to be small. The tabulated effective momentum transfers $q_{\rm eff}$ are for elastic scattering. The form factor for the 1.01 MeV peak belongs to an unresolved doublet consisting of the 1.005 and 1.020 MeV states.

E_0 (MeV)	$q_{\rm eff}$ (fm^{-1})	0.000 MeV $J^\pi = \frac{1}{2}^+$	0.159 MeV $\frac{3}{2}^+$	0.317 MeV $\frac{11}{2}^-$	0.712 MeV $\frac{7}{2}^+$	1.01 MeV $\frac{3}{2}^+, \frac{5}{2}^+$	1.18 MeV $\frac{5}{2}^+$	1.45 MeV	1.57 MeV
100.1	1.08	7.44 (49)	3.46 (97)	20.0 (12)	0.51 (202)	2.32 (43)	1.47 (81)	1.75 (94)	7.40 (22)
120.6	1.31	9.19 (21)	0.75 (258)	5.37 (24)	7.70 (17)	1.76 (54)	2.27 (47)	1.57 (97)	7.85 (20)
140.5	1.52	-1.75 (240)	1.67 (84)	1.93 (47)	14.2 (12)	3.13 (40)	3.38 (35)	1.56 (79)	4.35 (26)
160.9	1.74	1.18 (123)	1.59 (115)	17.5 (10)	9.50 (16)	1.08 (95)	1.11 (77)	1.05 (118)	5.88 (20)
170.8	1.85	4.24 (28)	2.89 (72)	22.7 (9)	6.49 (20)	1.31 (67)	0.54 (171)	<1	4.99 (19)
181.4	1.96	9.29 (30)	5.38 (65)	14.7 (21)	4.38 (42)	3.21 (42)	1.12 (116)	<3	6.29 (28)
200.7	2.17	9.11 (36)	8.94 (39)	4.48 (66)	2.10 (75)	8.96 (26)	1.76 (135)	3.60 (57)	4.78 (44)
221.2	2.39	8.10 (36)	8.57 (37)	1.96 (130)	6.13 (34)	10.6 (27)	3.91 (75)	1.70 (143)	6.50 (36)

given the relatively closely spaced single-particle levels in the $1g_{7/2}2d_{5/2}2d_{3/2}3s_{1/2}1h_{11/2}$ space, the "perturbative" CP approach cannot be expected to accurately describe the effects of the residual interaction in the $0\hbar\omega$ space.

In order to address this problem, the third model uses a full diagonalization of the residual interaction within the $0\hbar\omega$ shell-model space (the proton shell is left closed). All configurations within the $1g_{7/2}2d_{5/2}2d_{3/2}3s_{1/2}1h_{11/2}$ space were included, subject to the condition that no more than two neutrons be allowed in the $1h_{11/2}$ orbits. The interaction used in this space was the G matrix of Baldridge and Vary [18] as modified by Haxton, Stephenson, and Strottman [19] for the Te isotopes. The single-particle energies were adjusted slightly to improve the description of the low-lying spectrum. No reasonable set of single-particle energies could be found that resulted in a $\frac{1}{2}^+$ ground state. The simplistic IPM configuration $1g_{7/2}^{8\nu}2d_{5/2}^{6\nu}2d_{3/2}^{3\nu}$ dominated, and the predicted ground-state spin remained $\frac{3}{2}^+$ even when the full effects of configuration mixing were included. The calculated spectrum resulting from the final choice of shell-model parameters was $\frac{3}{2}^+$ (g.s.), $\frac{1}{2}^+$ (0.068 MeV), $\frac{11}{2}^-$ (0.385 MeV, fitted relative to the $\frac{1}{2}^+$ state), $\frac{7}{2}^+$ (0.571 MeV), $\frac{5}{2}^+$ (0.698 MeV), $\frac{3}{2}^+$ (1.002 MeV), and $\frac{5}{2}^+$ (1.111 MeV). Occupation probabilities for these states are listed in Table II.

The final approach is based upon these shell-model calculations, but included as well all first-order CP contributions involving configurations of $2\hbar\omega$ or greater excitation. This was carried out by means of an r-space Green's function technique [3]. Again the M3Y interaction was used for the CP calculations. The occupancies of the j shells in the $0\hbar\omega$ neutron space predicted from the shell-model calculations were used to weight the CP contributions for particle excitation out of this space into the higher empty shells as well as to determine the degree of blocking of excitation of particles from the closed neutron core into the $0\hbar\omega$ space. While any such composite calculation will not be entirely rigorous, we believe that this approach merges the key features of the shell-model calculations and CP and thus provides the most realistic description of the four that we consider.

IV. RESULTS AND INTERPRETATION

A. Elastic $M1$ form factor

Figure 2 shows the experimental results for elastic $M1$ scattering from ^{117}Sn. Coulomb scattering contributions from the nuclear charge distribution have been subtracted. The data are plotted as a function of the "effective" momentum transfer [20], in this case given by $q_{\text{eff}} = 1.07q$, where q is the three-momentum transfer

TABLE II. Calculated occupation probabilities for $0\hbar\omega$ shell-model configurations $1g_{7/2}^{a}2d_{5/2}^{b}2d_{3/2}^{c}3s_{1/2}^{d}1h_{11/2}^{e}$. The values have been summed over intermediate spin and isospin couplings. Included are only those configurations that contribute 5% or more to the occupancy of at least one level.

a	b	c	d	e	$\frac{3}{2}^+$	$\frac{1}{2}^+$	$\frac{11}{2}^-$	$\frac{7}{2}^+$	$\frac{5}{2}^+$	$\frac{3}{2}^+$	$\frac{5}{2}^+$
8	6	3	0	0	0.514					0.075	
8	6	2	1	0	0.002	0.463			0.014	0.200	0.523
8	6	2	0	1			0.465				
8	6	1	2	0	0.090					0.213	
8	5	4	0	0					0.414		0.007
8	5	3	1	0	0.003	0.011		0.002	0.003	0.189	0.123
8	5	2	2	0		0.004			0.188	0.014	0.074
8	5	2	0	2	0.003	0.002			0.059	0.004	0.005
8	4	4	1	0	0.002	0.171			0.004	0.001	0.003
8	4	4	0	1			0.183				
8	4	3	2	0	0.093	0.003			0.003	0.039	0.015
8	4	2	2	1			0.100				
8	4	2	1	2		0.050			0.001	0.011	0.026
8	3	4	2	0					0.058	0.002	0.005
7	6	4	0	0				0.384			
7	6	2	2	0				0.214		0.005	0.026
7	4	4	2	0				0.114			0.001
6	6	4	1	0		0.123			0.002	0.007	0.005
6	6	4	0	1			0.070				
6	6	3	2	0	0.072					0.034	0.003
6	6	3	0	2	0.067					0.006	0.001
6	6	2	1	2		0.073			0.002	0.023	0.056
6	5	4	2	0					0.066		0.007
6	5	4	0	2				0.004	0.058		
5	6	4	2	0				0.061			
		Calculated energy (MeV)			0.000	0.068	0.385	0.571	0.698	1.002	1.111
		Observed energy (MeV)			0.159	0.000	0.317	0.712	1.020	1.005	1.179

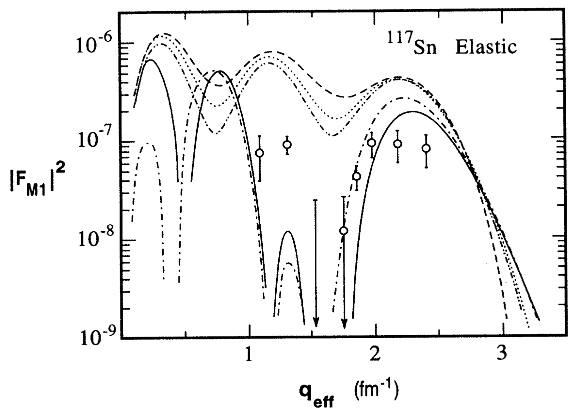

FIG. 2. Elastic $M1$ form factor of ^{117}Sn. The data are compared to various theoretical predictions. The dotted curve represents the results of an IPM calculation that employed radial wave functions derived from a harmonic oscillator well having size parameter b = 2.26 fm. When a Woods-Saxon potential well (R_0 = 1.22 fm, a = 0.60 fm) is used, the dashed curve is obtained. The dashed–double-dotted curve shows the IPM harmonic oscillator result when MEC's are included. Also shown are two core polarization calculations, both of which use harmonic oscillator wave functions. The dashed-dotted curve includes first-order CP, whereas the solid curve combines $0\hbar\omega$ shell-model configuration mixing with first-order CP to configurations with $2\hbar\omega$ or greater excitation energy.

from the electron. The applicability of this expression, established by directly comparing theoretical form factors calculated in plane-wave and distorted-wave Born approximations, simplifies the comparison of the data with the predictions of theoretical models.

Irrespective of the use of harmonic oscillator or Woods-Saxon radial wave functions, the IPM predictions are much larger than the data throughout the entire momentum transfer range of the measurements. In particular, the IPM totally fails to predict the deep diffraction minimum seen in the data near $q_{\rm eff}$ = 1.6 fm^{-1}. Furthermore, even though the IPM correctly locates a form factor maximum near $q_{\rm eff}$ = 2.3 fm^{-1}, the magnitude of the calculation exceeds the data by a factor of 5. Clearly, discrepancies of this order cannot be simply attributed to uncertainties in the form of the $3s_{1/2}$ radial wave function.

As indicated in Fig. 2, the inclusion of MEC's reduces the IPM harmonic oscillator result by 6% at $q_{\rm eff}$ = 2.3 fm^{-1} and by about 16% for the diffraction maxima at lower momentum transfer. This reduction contrasts with results obtained for most other magnetic form factors, where the theoretical predictions are *increased* when MEC's are included. In common with previous MEC evaluations [5, 21], the present calculation includes the pionic and pair exchange currents, as well as processes in which the $\Delta_{3,3}$ resonance is excited. The first two terms interfere constructively with the single-nucleon contribution. However, for ^{117}Sn this increase is negated by destructive interference with the resonance term. The overall reduction from the simple IPM prediction is characteristic of transitions that rely primarily on s-shell orbits, where the effects of the pair and pionic currents are diminished [21, 22]. Nevertheless, as is apparent from Fig. 2, the extent of the reduction brought about by MEC's is much smaller than that required to obtain agreement with the data.

As a further attempt to resolve the discrepancy, detailed shell-model evaluations were made, as described above, of the effects of $0\hbar\omega$ configuration mixing within the half-occupied neutron shell. Although not shown in Fig. 2, the $M1$ form factor obtained from these calculations differs only slightly from the corresponding IPM harmonic oscillator prediction. The q dependences are essentially identical, and the magnitude of the shell-model result is generally only 15% smaller than the IPM prediction. This slight reduction in the shell-model calculation derives mainly from a simple decrease in the occupation of configurations that have an unpaired $3s_{1/2}$ neutron. Even though other $0\hbar\omega$ neutron transitions now become possible, these make minor contributions to the elastic $M1$ form factor; certainly they do not explain the presence of the deep diffraction minimum seen near $q_{\rm eff}$ = 1.6 fm^{-1}.

As in the case of ^{205}Tl, it is CP that proves to be responsible for the deep diffraction minimum observed near $q_{\rm eff}$ = 1.5 fm^{-1}. Two CP calculations are presented in Fig. 2. As previously described, one is an average of first-order CP calculations based on the IPM for ^{115}Sn and ^{119}Sn. The second and preferred calculation combines first-order CP excitations of $2\hbar\omega$ or greater with the form factor given by a shell-model evaluation of $0\hbar\omega$ configuration mixing in the valence neutron shell. For both calculations, the contributions of first-order CP are very large, and interfere destructively with $0\hbar\omega$ contributions throughout most of the momentum transfer range.

Although the CP calculations account for the the presence of the deep diffraction minimum near $q_{\rm eff}$ = 1.6 fm^{-1}, they underestimate the magnitude of the apparent diffraction maximum observed at lower $q_{\rm eff}$, near 1.2 fm^{-1}. The disagreement appears large, but almost complete cancellation of the shell-model and CP contributions for 1.1< $q_{\rm eff}$ <1.7 fm^{-1} makes the total form factor sensitive to small changes of either of these components. This dependence is particularly acute for off-diagonal (e.g., $2d_{5/2} \rightarrow 2d_{3/2}$) transitions. Similar sensitivities in the region of intermediate-q maxima have been observed for the elastic M1 form factors of ^{205}Tl and ^{207}Pb [5], as well as for the much lighter nucleus ^{19}F [21].

The observation of a diffraction maximum near $q_{\rm eff}$ = 1.2 fm^{-1} therefore provides a sensitive test of models for the structure of ^{117}Sn. Since the ^{205}Tl magnetic form factor is unmeasured for $q_{\rm eff}$ < 1.4 fm^{-1}, no counterpart for this maximum has yet been found in ^{205}Tl. The prospect of extending the ^{205}Tl data to lower momentum transfers is extremely discouraging because, even for 180° scattering, Coulomb cross sections at low q become orders of magnitude larger than their magnetic counterparts. The difference with ^{117}Sn derives from the fact that whereas magnetic scattering is proportional to the square of the nuclear dipole moment, and is therefore relatively Z independent, Coulomb scattering varies as Z^2.

At high q the inclusion of CP also modifies the shell-model results in the desired direction; however, the magnitude of the diffraction maximum near $q_{\rm eff} = 2.3$ fm^{-1} is still overestimated by roughly a factor of 2. As can be seen in Fig. 2, the MEC's contribution obtained in the IPM provides only a small correction in this region of momentum transfer. It is therefore unlikely that MEC's would explain the discrepancy even if evaluated in the full shell-model and CP space.

It is noteworthy that CP calculations also overpredict the magnitude of the diffraction maximum seen near $q_{\rm eff} = 2.0$ fm^{-1} in ^{205}Tl, again by about a factor of 2. This similarity with ^{117}Sn is striking because, even though the elastic $M1$ form factors of these nuclei are both strongly determined by the existence of an unpaired valence $3s_{1/2}$ nucleon, the lowest-order shell-model structures are, as previously noted, quite different. These observations underscore the remarkable collective effect that $2\hbar\omega$ and higher-energy configurations have in modifying the IPM prediction.

Papanicolas *et al.* [1] have argued that within the $0\hbar\omega$ space the $3s_{1/2} \rightarrow 3s_{1/2}$ single-particle matrix element is dominant at large q because of the relatively rapid oscillations of the $3s_{1/2}$ wave function in coordinate space. This being the case, the magnitude of the $M1$ form factor in the vicinity of the last observed diffraction maximum should be primarily determined by the amplitudes of configurations that have an unpaired $3s_{1/2}$ neutron. The results of the calculations shown in Fig. 2 indicate that the combination of theoretical effects explored here still overestimates the strength of such configurations. In part, this failure may be due to the neglect of multiparticle-multihole correlations which have the potential to further fragment or diminish the amplitudes of configurations in which there is an unpaired $3s_{1/2}$ neutron. As previously noted, for nuclei in the vicinity of ^{208}Pb, Pandharipande, Papanicolas, and Wambach [6] and Benhar, Fabrocini, and Fantoni [7] showed that the occupation probability of orbits just below the Fermi energy should be reduced by correlations to about 0.7. Similarly, a satisfactory explanation of the ^{117}Sn data may rely upon the evaluation of second- and higher-order core polarization, i.e., multiparticle-multihole configurations outside the $0\hbar\omega$ basis space.

B. Inelastic transverse form factors

Figures 3 and 4 show form factors corresponding to inelastic peaks observed at 0.159, 0.317, 0.712, 1.01, 1.18, and 1.57 MeV. The peak at 1.01 MeV arises from unresolved excitations of the doublet consisting of the known 1.005 MeV ($J^\pi = \frac{3}{2}^+$) and 1.020 MeV ($\frac{5}{2}^+$) states. No interpretation has been attempted for the 1.57 MeV peak associated with a multiplet of states, most of which have uncertain spin and parity assignments. A similar unresolved multiplet may be responsible for a weak peak at 1.45 MeV, the form factor for which is given in Table I. The results for the 1.45 MeV and 1.57 MeV excitations will not be discussed further.

Unlike the elastic form factor, which is pure $M1$, transverse form factors for the inelastic transitions consist of incoherent sums of magnetic and electric multipoles. For example, the form factor of the 0.159 MeV transition contains $M1$ and $E2$ components, the 0.317 MeV form factor is a sum of $E5$ and $M6$, and $M3$ and $E4$ multipoles make up the 0.712 MeV transition. In general, both the IPM and the shell model provide a reasonable description of the shapes of the inelastic form factors. In the IPM, the electric and magnetic components of each of these three excitations have identical form factor shapes; the shell model does not preserve these identical q dependences,

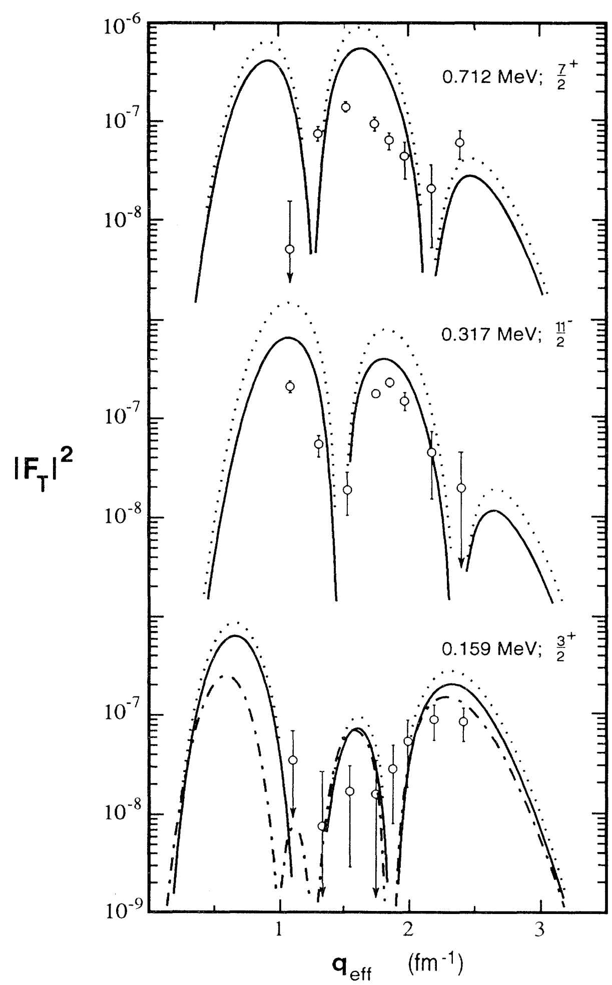

FIG. 3. Inelastic form factors for the 0.159 MeV ($M1$+$E2$), 0.317 MeV ($E5$+$M6$), and 0.712 MeV ($M3$+$E4$) transitions in ^{117}Sn. Longitudinal scattering contributions have not been subtracted from the data, but are estimated to be small. The dotted curves indicate transverse form factors given by the IPM, whereas solid curves show the results of $0\hbar\omega$ configuration-mixed shell-model calculations. For the transition to the 0.159 MeV level, the dashed-dotted curve combines the shell-model prediction with a CP contribution as described in the text.

but the differences are small. For the 0.159 MeV transition the $E2/M1$ form factor ratio is equal to 3 in the IPM vs about 2.8 in the shell model; for the 0.317 and 0.712 MeV transitions the $M6/E5$ and $E4/M3$ ratios are 7/5 vs 1.3 and 5/3 vs 1.8, respectively.

The curves shown in Fig. 3 represent the IPM and shell-model predictions for these transitions, calculated using harmonic oscillator radial wave functions. Similar observations may be made for each of the three cases. Although their diffraction structures are essentially correct, the IPM predictions are generally much larger than the data. More detailed shell-model calculations give results that are 25–50 % less than the IPM predictions, but these still exceed the data by factors of 2–4. Similar results are obtained for the form factor of the 1.01 MeV doublet, shown in Fig. 4. According to the shell-model calculations, it is the transition to the $J^\pi = \frac{5}{2}^+$ state which accounts for most of the cross section observed for this peak.

Note that the IPM calculation shown at the bottom of Fig. 4 represents the total form factor obtained for $3s_{1/2} \to 2d_{5/2}$ transitions with harmonic oscillator wave functions. Because the IPM predicts only one low-lying $J^\pi = \frac{5}{2}^+$ state, the corresponding $E2$ and $M3$ excitation strength should be fragmented between the two $\frac{5}{2}^+$ levels observed at 1.020 and 1.18 MeV. As indicated in Fig. 4, the shell model is fairly successful in predicting this fragmentation. The 1.18 MeV state has a more complex, configuration-mixed structure, and hence in this case the $E2$ and $M3$ components predicted by the shell model exhibit somewhat different q dependences.

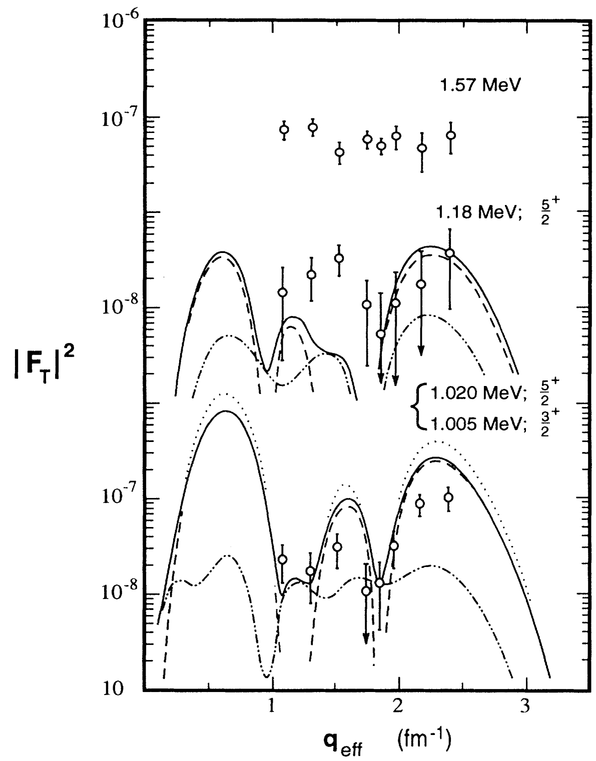

FIG. 4. Inelastic form factors for higher-excited states in ^{117}Sn. Data at the bottom are for the unresolved doublet consisting of the 1.005 MeV ($M1$+$E2$) and 1.020 MeV ($E2$+$M3$) transitions. The dotted curve represents the IPM prediction for $3s_{1/2} \to 2d_{5/2}$ neutron transitions. All other curves in this figure result from $0\hbar\omega$ configuration-mixed shell-model calculations. For the 1.01 MeV doublet, the dashed–double-dotted curve belongs to the 1.005 MeV transition, the dashed curve to the 1.020 MeV transition, and the solid curve is the sum. For the 1.18 MeV transition, the dashed–double-dotted curve shows the E2 contribution, the dashed curve the M3 contribution, and the solid curve is the sum. All calculations used single-particle radial wave functions derived from a harmonic oscillator potential well.

Given the evident importance of first-order CP in the elastic $M1$ form factor, consideration of CP might also be expected to yield an improved understanding of the inelastic transverse form factors. As an example, consider the form factor for excitation of the 0.159 MeV $\frac{3}{2}^+$ state. In this case about half of the shell-model prediction for the form factor comes from the IPM transition $1g_{7/2}^8 2d_{5/2}^6 2d_{3/2}^2 3s_{1/2} \to 1g_{7/2}^8 2d_{5/2}^6 2d_{3/2}^3$ and this provides a starting point for a CP calculation. In order to assess the influence of CP in this excitation we have used the final method discussed in Sec. III to evaluate CP based on this single-particle component only. This contribution was then reduced by the appropriate shell-model amplitude and added to the shell-model form factor. As shown in Fig. 3, the inclusion of this CP component generally reduces the calculated form factor, as required by the data. However, as indicated in Table II, other $0\hbar\omega$ components make appreciable contributions to this excitation. CP excitations based on these smaller, neglected components would likely combine to produce further significant modifications of the calculated form factor. Exploratory attempts to evaluate CP contributions for other inelastic transitions also tended to decrease the predicted form factors, therefore improving agreement with the data.

V. CONCLUSIONS

The data reported here for the elastic $M1$ form factor of ^{117}Sn seem to support a similar interpretation as that of previous measurements of elastic magnetic scattering from ^{205}Tl and ^{207}Pb. That is, simple independent-particle model or $0\hbar\omega$ shell-model descriptions fail to describe the $M1$ form factor. Multi-$\hbar\omega$ first-order core polarization is needed to explain the most prominent feature of the form factor, namely, the deep diffraction minimum at intermediate q. Even then, however, the calculations overestimate by a factor of approximately 2 the magnitude of the form factor maximum at high q, suggesting, as for ^{205}Tl and ^{207}Pb, the need to include further depletion of the occupation probability near the Fermi surface. Comparisons with the data for the first few inelastic transitions qualitatively support the validity of the shell model, but only as a starting point: The results of our exploratory calculations suggest that CP is also significant for inelastic transitions. In order to confirm these conclusions there is a need for more complete and consistent calculations that include not only first-order CP, but also the effects of multiparticle-multihole excitations outside the $0\hbar\omega$ space.

ACKNOWLEDGMENTS

We are grateful to Dr. Ravi P. Singhal who first suggested this experiment. This work was supported by the U.S. Department of Energy under Grant No. DE-FG02-88ER40415. A.H. and T.S. gratefully acknowledge the financial assistance of the Japanese Ministry of Education under a grant from the Monbusho International Scientific Research Program.

[1] C. N. Papanicolas, L. S. Cardman, J. H. Heisenberg, O. Schwentker, T. E. Milliman, F. W. Hersman, R. S. Hicks, G. A. Peterson, J. S. McCarthy, J. Wise, and B. Frois, Phys. Rev. Lett. **58**, 2296 (1987).

[2] I. Hamamoto, J. Lichtenstadt, and G. Bertsch, Phys. Lett. **93B**, 213 (1980).

[3] T. Suzuki, M. Oka, H. Hyuga, and A. Arima, Phys. Rev. C **26**, 750 (1982).

[4] G. Bertsch, J. Borysowicz, H. McManus, and W. G. Love, Nucl. Phys. **A284**, 399 (1977).

[5] T. Suzuki and H. Hyuga, Nucl. Phys. **A402**, 491 (1983).

[6] V. R. Pandharipande, C. N. Papanicolas, and J. Wambach, Phys. Rev. Lett. **53**, 1133 (1984).

[7] O. Benhar, A. Fabrocini, and S. Fantoni, Phys. Rev. C **41**, R24 (1990).

[8] E. J. Schneid, A. Prakash, and B. L. Cohen, Phys. Rev. **156**, 1316 (1967).

[9] C. R. Bingham and M. L. Halbert, Phys. Rev. C **1**, 244 (1970).

[10] G. A. Peterson, J. B. Flanz, D. V. Webb, H. de Vries, and C. F. Williamson, Nucl. Instrum. Methods **160**, 375 (1979).

[11] W. Bertozzi, M. V. Hynes, C. P. Sargent, W. Turchinetz, and C. F. Williamson, Nucl. Instrum. Methods **162**, 211 (1979).

[12] R. S. Hicks, A. Hotta, J. B. Flanz, and H. de Vries, Phys. Rev. C **21**, 2177 (1980).

[13] F. Borkowski, P. Penser, G. G. Simon, V. H. Walther, and R. D. Wending, Nucl. Phys. **A222**, 269 (1974).

[14] R. E. Rand, Nucl. Instrum. Methods **39**, 45 (1966).

[15] A. Hotta, R. S. Hicks, R. L. Huffman, G. A. Peterson, R. J. Peterson, and J. R. Shepard, Phys. Rev. C **36**, 2212 (1987).

[16] T. E. Milliman, Ph.D. dissertation, University of New Hampshire, 1987 (unpublished).

[17] J. R. Ficenec, L. A. Fajardo, W. P. Trower, and I. Sick, Phys. Lett. **42B**, 213 (1972).

[18] W. J. Baldridge and J. P. Vary, Phys. Rev. C **14**, 2246 (1976).

[19] W. C. Haxton, G. J. Stephenson, Jr., and D. Strottman, Phys. Rev. D **25**, 2360 (1982).

[20] D. G. Ravenhall and D. R. Yennie, Proc. Phys. Soc. London A **70**, 857 (1957).

[21] A. J. H. Donne, B. van Middelkoop, L. Lapikas, T. Suzuki, P. W. M. Glaudemans, and D. Zwarts, Nucl. Phys. **A455**, 453 (1986).

[22] I. S. Towner and F. C. Khanna, Nucl. Phys. **A399**, 334 (1983).